Improved identification could be achieved if the parent gases are removed by cryogenic cooling. Samples and controls were kept shielded from sunlight and room light. No measurable production of organics was found in the controls.
17. The solid residue was analyzed by solution in boiling dichloromethane and in methanol. No organic material was detected at a level of 1 ppm in the dichloromethane. The methanol solution, examined with a Fourier Transform Infrared Spectrometer (IBM model 32), indicated the presence of soluble organic matter. Infrared absorption bands were identified at 2922, 2855, and 1450 wavenumbers, indicating the presence of aliphatic hydrocarbons; at 1516 wavenumbers, indicating a small amount of aliphatic amine; at 1636 wavenumbers, indicating an amide group; and at 1117 wavenumbers, indicating the possible presence of alcohol groups. We could not accurately determine the yield of the solid residue because of the long exposure time required to produce this material and the resulting reprocessing of products. However, based on the exposure time (20 min) and product amount (determined to be about 0.01 mg on the basis of concentrations in solution), we can estimate its yield at about 1% of the yield of the major hydrocarbons. An x-ray fluorescence spectrum of the solid residue showed a strong sulfur line, indicating incorporation at the few percent level in the solid residue.
18. We estimated the importance of UV production, using the results of experiments in which the shock is isolated from the parent mixture by a UV transparent window (*6*). Yields of the main photolysis products with UV-only compared to yields with complete shocks were: 1 to 4% C_2H_2, 10 to 20% C_2H_6, and 0.1 to 1% HCN. Our results correspond to similar yields for the UV production, ≃1 to 10% of the total shock production is due to UV.
19. Y. L. Yung, M. Allen, J. P. Pinto, *Astrophys. J. Suppl. Ser.* **55**, 465 (1984).
20. J. B. Pollack, Y. L. Yung, *Annu. Rev. Earth Planet. Sci.* **8** 425 (1980); H. D. Holland, *The Chemical Evolution of the Atmosphere and Oceans* (Princeton Univ Press, Princeton, NJ, 1984).
21. L. M. Mukhin, M. V. Gerasimov, E. N. Safonova, *Nature* **340**, 46 (1989).
22. We can compare the expected yields for organics on early Earth with the other main production mechanism, solar UV light. C. Chyba and C. Sagan [*Nature* **355**, 125 (1992)] estimate that the solar UV produces 3×10^8 kg year^{-1} in a neutral atmosphere and 2×10^{11} kg year^{-1} in a reducing atmosphere. For our CH_4-containing mixture and using the atmospheric shock deposition rate estimated by Chyba and Sagan of 10^{17} J year^{-1}, we find an organic production of 3×10^{10} kg year^{-1}. For the lightning rate of Chyba and Sagan, 10^{18} J year^{-1}, the organic production is 3×10^{11} kg year^{-1}.
23. W. J. Borucki, R. L. McKenzie, C. P. McKay, N. D. Duong, D. S. Boac, *Icarus* **64**, 221 (1985); W. J. Borucki and C. P. McKay, *Nature* **328**, 509 (1987).
24. W. J. Borucki, C. P. McKay, R. S. Rogers, D. S. Boac, N. D. Duong, J. E. Parris, *Appl. Opt.* **26**, 4319 (1987).
25. A. H. Delsemme, *Philos. Trans. R. Soc. London Ser. A* **325**, 509 (1988). Some 10% of the O_2 has been removed to account for oxides in the rock fraction of the cometary material, as in D. Simonelli, J. B. Pollack, C. P. McKay, R. T. Reynolds, and A. L. Summers [*Icarus* **82**, 1 (1989)].
26. This research was supported by subventions from the NASA Exobiology Program. We thank M. Carter of Carter Analytical Laboratories for performing the GC-MS analysis and for helpful discussions. GC analysis was performed by D. Kojiro, F. Church, and R. Quinn.

17 October 1996; accepted 19 February 1997

Giant Piezoelectric Effect in Strontium Titanate at Cryogenic Temperatures

Daniel E. Grupp and Allen M. Goldman*

Piezoelectric materials have many applications at cryogenic temperatures. However, the piezoelectric response below 10 kelvin is diminished, making the use of these materials somewhat marginal. Results are presented on strontium titanate ($SrTiO_3$), which exhibits a rapidly increasing piezoelectric response with decreasing temperature below 50 kelvin; the magnitude of its response around 1 kelvin is comparable to that of the best materials at room temperature. This "giant" piezoelectric response may open the way for a broad class of applications including use in ultralow-temperature scanning microscopies and in a magnetic field–insensitive thermometer. These observations, and the possible divergence of the mechanical response to electric fields at even lower temperatures, may arise from an apparent quantum critical point at absolute zero.

The phenomenon of piezoelectricity, as a solid-state method for converting electrical signals into mechanical motion, has become ubiquitous in its applications in the laboratory as well as in everyday life. Its elegant simplicity is evident in such varied uses as the beeping of a watch and the ultrasensitive micropositioning required to arrange individual atoms on a surface. However, it is not without limitations. In particular, the piezoelectric response is typically reduced by orders of magnitude at cryogenic temperatures. We have found an important exception to this in the crystal $SrTiO_3$ (STO), for which the piezoelectric response grows at low temperature and at 1.6 K is comparable to that of the best materials at room temperature.

We present results from measurements of the electric field–induced strain in single crystals of STO in the temperature range $T = 1.6$ to 50 K. This material is one of the most widely studied in condensed-matter physics, exhibiting a variety of phenomena including structural phase transitions (*1*) which have been calculated recently from first principles (*2*), the rare phenomenon of second sound (*3*), and the identification of a low-temperature quantum paraelectric (QPE) ground state by Müller and Burkard (*4*). It is the latter which underlies the phenomena in our investigations.

The electric field–induced (*5*) and pressure-induced (*6*) strain in STO has been investigated since the early 1960s, but the observations were confined to a few temperatures and voltages. In this work, we have mapped out a full surface in voltage and temperature, which reveals behavior much richer than previously thought (Fig. 1). Perhaps the most important feature of the data is the strong increase in the magnitude of the electric field–induced strain S as T is decreased. The strain S is the relative change in length, $\Delta\ell/\ell$ along $\hat{x}$ for a field $\mathbf{E} = E\hat{z}$. By contrast, standard piezoelectric ceramics such as lead zirconate titanate (PZT) would exhibit a strain of the order 10 microstrain at our lowest temperature for the same sample geometry. Further, the strain in PZT decreases as T is lowered, whereas the strain in STO increases.

The experiments were performed on a single-crystal substrate of STO, 10 mm by 10 mm by 0.75 mm, from Princeton Scientific. The impurities were determined by the manufacturer (*7*). We measured S using a foil strain gauge from Omega Engineering (model SG-LY11). The gauge was bonded with cyanoacrylate (Omega) after the faces of the crystal had been coated with 500 Å of chrome. Calibration of the gauge was based on measurements on commercially available PZT with typical strain versus temperature characteristics. Thus, although the precision of the gauges is better than 10^{-7} strain, the accuracy is only about 20%.

At low voltages, the strain is quadratic in the voltage (Fig. 2), characteristic of a paraelectric (PE). In this regime, S for a field E is given by

$$S_{ij} = R_{kij}E_k^2 \quad (1)$$

where the coefficient of electrostriction, $\mathbf{R}$, is a fourth-rank tensor, with $i, j = 1$ to 3 and $k = 1$ to 6 in a double-index form (*8*). Above a crossover voltage V_c associated with a crossover field E_c (voltage is the measured quantity and it is simply related to the field E through the crystal thickness, $t = 0.75$ mm), the strain is linear in field, characteristic of a piezoelectric, with

$$S_{ij} = d_{kij}E_k \quad (2)$$

where the piezoelectric coefficient, $\mathbf{d}$, is a third-rank tensor (*8*), with $i, j, k = 1$ to 3. We always applied E_3 and measured R_{311} and d_{311} (*9*).

School of Physics and Astronomy, University of Minnesota, Minneapolis, MN 55455, USA.

*To whom correspondence should be addressed.

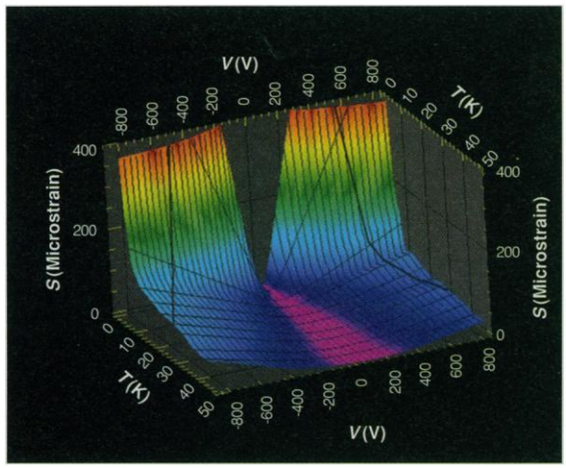

Fig. 1. Electric field–induced strain as a function of temperature and voltage in STO. The rapid increase of S makes this material a leading candidate for piezoelectric applications at low temperature. The linear region outside of the heavy black lines has been extrapolated in plotting the surface. This corner of the graph may exhibit saturation, as explained in the text. The color is proportional to the value of the strain S, with violet indicating low and red indicating high. (Graphics: B. F. Schaudt, University of Minnesota Supercomputer Institute.)

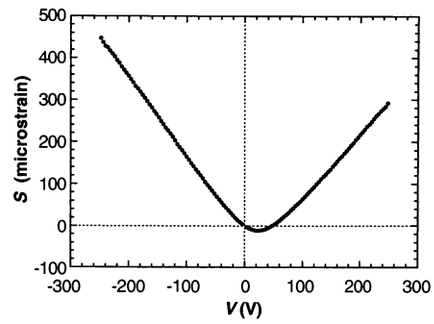

Fig. 2. Electric field–induced strain in STO as a function of voltage at our lowest temperature, T = 1.6 K. The response is quadratic at low fields, characteristic of a PE, and linear at high fields, characteristic of a piezoelectric. The strain is large compared to that of other commonly used materials at this temperature. The voltage is also lower than that typically used, making this material an excellent choice for many applications.

The results for the coefficients as a function of temperature are plotted in Fig. 3. Both the electrostriction and the piezoelectric effect diverge as power laws in T, with $R_{311} \simeq 1/T^2$ and $d_{311} \simeq 1/T$. Further, analysis appears to show that they are asymptotic to $T = 0$. The practical implication is that the response remains large and may actually continue to grow, down to absolute zero. At our lowest temperature (T = 1.6 K), the coefficients are $R_{311} = 14.5 \times 10^{-15}$ m^2/V^2 and $d_{311} = 16 \times 10^{-10}$ m/V. These values are comparable in magnitude to those of PZT at room temperature, whereas at 4.2 K in PZT, d_{311} can be as high as 5×10^{-10} m/V and is significantly lower at T = 1.6 K (Fig. 3, inset). To our knowledge, this result makes STO the material with the largest piezoelectric response currently available for low-temperature use. The compound, lithium thallium tartrate (LTT), $LiTlC_4H_4O_6 \cdot H_2O$, has a larger piezoelectric coefficient at T = 10 K, which is its ferroelectric transition temperature (*10*). Because piezoelectric coefficients peak at ferroelectric transitions, one might expect that with decreasing temperature the piezoelectric coefficient of LTT would fall below that of STO, which is diverging with decreasing temperature.

The diverging behavior of the electromechanical response of STO is at first counterintuitive. As the PZT crystal cools, thermal fluctuations die out and electromagnetic forces dominate, with a corresponding decrease in piezoelectric response and elasticity. Essentially, the crystal hardens. In STO, however, the increasing electrostrictive response implies that the crystal softens as the temperature is lowered. It is known through measurements of the dielectric constant ϵ as a function of T that STO begins to exhibit a ferroelectric (FE) transition (ϵ diverges) with a Curie temperature of $T_c \simeq 35$ K (*11*) but instead becomes a QPE (ϵ flattens out around 10 K) (*4*). The QPE is characterized by zero-point motion of the Ti atoms. These quantum fluctuations effectively suppress the FE transition to $T = 0$, as supported in recent first-principles calculations (*2*). Recent experiments have found indications that there is a $T = 0$ electric field–driven phase transition from a PE to a piezoelectric state that is possibly an FE (*12*). This quantum critical point at $T = 0$ may be associated with the apparent divergent response. As the temperature is lowered, the system approaches more closely the neighborhood of the quantum critical point. Thus, although the reduction of the response in PZT as the temperature is lowered arises from decreasing classical thermal fluctuations, the growing piezoelectric response in STO may arise from the approach to the quantum critical point.

The magnitude of the strain is not without bound. At higher voltages than shown in Fig. 2, S saturates, that is, becomes constant with further increase in voltage. This is a common effect in piezoelectrics, where the forces from the fields between ions in the crystal dominate the forces from the applied field. Still, the geometry we tested yielded a maximum extension of 5 μm/cm, which is considerable. Other standard geometries such as tubes or bilayers could be used to produce greater travel.

Another issue is that of domains. These may arise when the perovskite crystal passes through the structural phase transition at 105 K, going from cubic to tetragonal. In the tetragonal phase, there is an elongation of the cubic cell along the c axis, a direction normal to one of the faces. Symmetry dictates that the c axis may lie in any of three equivalent orthogonal directions. A domain with the c axis parallel to $\hat{x}$ in the plane of our crystal will then exert a lateral force on a neighboring domain in that direction and a shear force on a domain in the $\hat{y}$ direction. The crystal is then strained with no applied voltage.

The shear breaks the centrosymmetric symmetry and may result in an offset in voltage of the minimum strain. Such an asymmetry may also arise from crystal defects. In our sample, we observe an offset that moves from 70 V at 50 K to about 25 V at 1.6 K, with an offset in strain of $S_{off} \simeq 1$ microstrain (Fig. 2). This may result from a change in the internal strain with T, as the structural phase transition is second order, so the tetragonal distortion grows continuously to $T = 0$ (*13*). However, the domains themselves do not change with temperature and are unaffected by applied fields (*14*). It has been reported that it may be possible to remove the domains by thermal cycling (*4*) or by using sufficiently thin plates (*15*). This removal would simplify the operation of any device that depended on the behavior around zero volts. Without removing the domains, the minimum in S would have to be found after cooldown, and the apparatus would need to be adjusted accordingly.

Also of practical interest is an apparent lack of hysteresis in S upon cycling of V. The

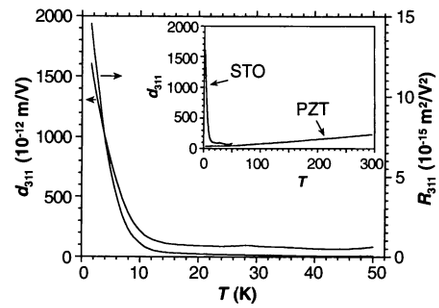

Fig. 3. Coefficients of electrostriction, R_{311}, and piezoelectricity, d_{311}, in STO versus T. Both diverge as inverse power laws of temperature and are comparable in magnitude to the coefficients of high-performance materials at room temperature. The inset shows the measured piezoelectric coefficient of a sample of PZT compared with that for STO.

curves of S versus V are highly reproducible and independent of voltage history. If there is any hysteresis, it is much less than 1 microstrain.

Two primary areas where STO may find application are in low-temperature actuators and magnetic field–insensitive thermometers. The most broadly used application for linear actuators is in cryogenic scanning probe microscopy (*16–19*). The linear (piezoelectric) region above V_c is most useful here. Operation would then be about a bias voltage, which near 4.2 K is only about $V_c = 25$ V. The absence of hysteresis also makes precise scanning simpler, although the temperature dependence of the effect would require significant temperature stabilization. The phase boundary separating quadratic from linear behavior is shown in Fig. 4. The crossover voltage decreases with T and shows no sign of flattening out. This effect is useful for linear applications, which would then require a smaller bias voltage at lower T. At V_c, the value of the strain S_c is actually increasing. Thus, any application that depends on the quadratic behavior continues to work as T is lowered but requires less voltage for the same response. Such applications might include acoustic generators (*20*), which would act as frequency doublers as a result of the quadratic response.

The divergence of the coefficients R and d may also be used as a thermometer. Because there are no spins or currents in STO at low temperatures, the main advantage of such a thermometer would be that it might be unaffected by a magnetic field, a very difficult property to achieve in cryogenic thermometry. A lock-in amplifier could be used with an ac applied voltage to continuously read the slope of the curve of S versus V. If a metal strain gauge were to be used (as in our experiment), although the resistance Ω may change in a magnetic field, the ratio $S = \Delta\Omega/\Omega$ would not change. Other methods of measuring the strain may be used as well. Given the apparent divergence of R, such a thermometer may work at temperatures far below what we have measured (*22*).

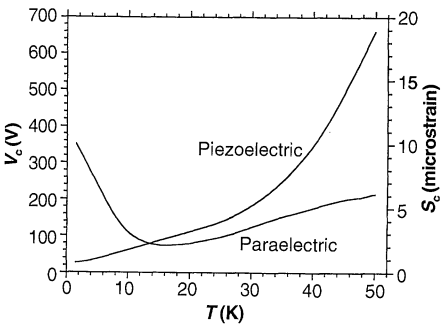

Fig. 4. The boundary between quadratic (PE) and linear (piezoelectric) behavior of the electric field–induced strain in STO shown as the value of the voltage V_c and strain S_c at the crossover as a function of temperature. At low temperatures S_c is increasing, implying that the PE region, which is useful in certain applications, persists to $T = 0$; the decreasing V_c shows that less voltage is required to reach the linear response regime (*21*).

REFERENCES AND NOTES

1. K. A. Waldner, W. Berlinger, F. Waldner, *Phys. Rev. Lett.* **21**, 814 (1968).
2. W. Zhong and D. Vanderbilt, *Phys. Rev. B* **53**, 5047 (1996).
3. B. Hehlen, A.-L. Pérou, E. Courtens, R. Vacher, *Phys. Rev. Lett.* **75**, 2416 (1995).
4. K. A. Müller and H. Burkard, *Phys. Rev. B* **19**, 3593 (1979).
5. G. Schmidt and E. Hegenbarth, *Phys. Status Solidi* **3**, 329 (1963).
6. H. Uwe and T. Sakudo, *Phys. Rev. B* **13**, 271 (1976).
7. Impurities (in parts per million) are as follows: Na < 2, K = 2, Al = 44, Si < 2, Ca = 14, Fe < 2, Ba = 19.
8. The index k goes from 1 to 6 to include the cases in which two orthogonal electric fields are applied, for example, $E_3^2 = E_3E_3$ and $E_4^2 = E_1E_3$ [see I. S. Zheludev, *Physics of Crystalline Solids* (Plenum, New York, 1971), vol. 2].
9. Because the linear regime occurs above a crossover field, it does not extrapolate to zero strain at zero field. Including the crossover fields, we have $S_{ij} \simeq S_{cij} + d_{kij}(E_j - E_{cj})$ (it is not exact because S_c and E_c are taken in the middle of the crossover). The main point is that the derivative of this form and Eq. 2 are both d_{kij}.
10. E. Sawaguchi and L. E. Cross, *Ferroelectrics* **2**, 37 (1971).
11. Y. Yamada and G. Shirane, *J. Phys. Soc. Jpn.* **26**, 396 (1969).
12. D. E. Grupp and A. E. Goldman, in preparation.
13. S. L. Sondhi, S. M. Girvin, J. P. Carini, D. Shahar, *Rev. Mod. Phys.*, in press. (available at http://xxx.lanl.gov at cond-mat/9609279).
14. E. Sawaguchi, A. Kikuchi, Y. Kodera, *J. Phys. Soc. Jpn.* **18**, 459 (1963).
15. K. A. Müller, W. Berlinger, M. Capizzi, H. Gränicher, *Solid State Commun.* **8**, 549 (1970).
16. G. Meyer, *Rev. Sci. Instrum.* **67**, 2960 (1996).
17. J. Siegel, J. Witt, N. Venturi, S. Field, *ibid.* **66**, 2520 (1995).
18. F. Mugele, C. Kloos, P. Leiderer, R. Moller, *ibid.* **67**, 4880 (1996).
19. J. A. Helfrich, S. Adenwalla, J. B. Ketterson, *ibid.* **66**, 4880 (1995).
20. I. C. Manzanares, N. Mina-Camilde, A. Brook, J. Peng, V. M. Blunt, *ibid.*, p. 2644.
21. The high-field regime is labeled piezoelectric and not FE because it is possible that noncentrosymmetric systems exhibiting piezoelectricity may not be FE. This question might be resolved by low-temperature measurements in an electric field of the crystal structure or polarization. Although data relating to the latter are in the literature, further experiments are needed to firmly establish the existence of a high-field FE state in STO [see J. Hemberger, P. Lunkenheimer, R. Viana, R. Böhmer, A. Loidl, *Phys. Rev. B* **52**, 13159 (1995)].
22. Some years ago, W. N. Lawless [*Ferroelectrics* **7**, 379 (1974)] developed an STO glass-ceramic that has been used as a low-temperature, magnetic field–insensitive capacitance thermometer because its dielectric constant is temperature-dependent. The proposed STO strain thermometer may ultimately be more useful because of the apparent divergence of the strain with decreasing temperature. The dielectric constant of $SrTiO_3$ glass is not strongly temperature-dependent at the lowest temperatures.

23. Supported in part by NSF under grant NSF/DMR-9623477.

26 December 1996; accepted 20 February 1997

Primary Production in Antarctic Sea Ice

Kevin R. Arrigo,* Denise L. Worthen, Michael P. Lizotte, Paul Dixon, Gerhard Dieckmann

A numerical model shows that in Antarctic sea ice, increased flooding in regions with thick snow cover enhances primary production in the infiltration (surface) layer. Productivity in the freeboard (sea level) layer is also determined by sea ice porosity, which varies with temperature. Spatial and temporal variation in snow thickness and the proportion of first-year ice thus determine regional differences in sea ice primary production. Model results show that of the 40 teragrams of carbon produced annually in the Antarctic ice pack, 75 percent was associated with first-year ice and nearly 50 percent was produced in the Weddell Sea.

Sea ice surrounding the Antarctic continent varies in extent from 4×10^6 km^2 in summer to 20×10^6 km^2 in winter (*1*) and represents one of the largest and most dynamic ecosystems on Earth. Algae associated with ice may attain standing crops with amounts of chlorophyll a in excess of 400 mg m^{-2} and rates of primary production of >1 g C m^{-2} day^{-1}, comparable to productive oceanic regions (*2*, *3*). Because sea ice microalgal production is spatially and temporally variable, its contribution to the carbon cycle of the Southern Ocean and its importance as a food source for higher trophic levels [such as overwintering juvenile krill (*4*)] have been difficult to determine.

We used an expanded version of a one-

K. R. Arrigo, NASA Oceans and Ice Branch, Goddard Space Flight Center, Code 971.0, Greenbelt, MD 20771, USA.
D. L. Worthen, Science Systems and Applications Inc., Lanham, MD 20706, USA.
M. P. Lizotte, Department of Biology and Microbiology, University of Wisconsin–Oshkosh, Oshkosh, WI 54901, USA.
P. Dixon, Scripps Institution of Oceanography, University of California, San Diego, La Jolla, CA 92093, USA.
G. Dieckmann, Alfred-Wegener Institut für Polar- und Meeresforschung, Columbusstrasse, D-27570 Bremerhaven, Germany.
*To whom correspondence should be addressed.